

# DESIGN OF 10 GEV LASER WAKEFIELD ACCELERATOR STAGES WITH SHAPED LASER MODES \*

E. Cormier-Michel, E. Esarey, C.G.R. Geddes, C.B. Schroeder, W.P. Leemans,  
Lawrence Berkeley National Laboratory, Berkeley CA, 94720, USA  
D.L. Bruhwiler, B. Cowan, K. Paul,  
Tech-X Corporation, Boulder CO, 80303, USA

*Abstract*

We present particle-in-cell simulations, using the VORPAL framework, of 10 GeV laser plasma wakefield accelerator stages. Scaling of the physical parameters with the plasma density allows us to perform these simulations at reasonable cost and to design high performance stages. In particular we show that, by choosing to operate in the quasi-linear regime, we can use higher order laser modes to tailor the focusing forces. This makes it possible to increase the matched electron beam radius and hence the total charge in the bunch while preserving the low bunch emittance required for applications.

## INTRODUCTION

Laser driven wakefield accelerators (LWFAs) are able to produce accelerating gradients thousands of times higher than conventional accelerators, making them suitable to build compact devices. In a LWFA the radiation pressure of the laser pulse induces charge separation, producing a plasma wave (wake) traveling at the group velocity of the laser pulse, close to the speed of light, and hence able to accelerate particles to relativistic velocities (see [1] for a complete review). Energies up to a GeV have been obtained in only a few centimeters [2]. Recently, experiments have shown that it is possible to control the injection and the acceleration of electrons [3, 4], providing a path towards high quality electron beams that can be used for applications, including free electron lasers [5], gamma ray sources [6] and colliders for high energy physics [7]. Light sources need stable electron bunches of the order of a GeV. A multi-TeV collider was designed using staging of several 10 GeV LWFA accelerator modules at a density of  $n_0 \sim 10^{17} \text{ cm}^{-3}$ , each about a meter long [7]. Efficient transfer of the laser energy to the accelerated beam, acceleration of positrons and conservation of a low emittance must be considered for applications. In this paper we present the design of these stages using Particle-In-Cell (PIC) simulations with the VORPAL framework [8]. We show that by using higher order laser modes, in the quasi-linear regime, the focusing forces in the wake can be controlled in order to improve the stage efficiency.

## RESULTS

The PIC method is a fully self-consistent algorithm which allows non-linear evolution of the plasma wake and of the laser pulse simultaneously. In PIC simulations the smallest dimension, i.e., the laser wavelength ( $\lambda \sim 1 \mu\text{m}$ ), needs to be resolved, whereas the box size increases with the plasma wave wavelength  $\lambda_p = (\pi c^2 m / e^2 n_0)^{1/2}$ , where  $n_0$  is the plasma density. The acceleration length also increases with higher energy stages, i.e., lower plasma densities, making the simulations more computationally intensive. Simulations of a 1 GeV stage, to model the recent experiments or gamma ray sources, with a density of  $n_0 \sim 10^{18} \text{ cm}^{-3}$ , require of the order of  $10^6$  processor-hours and  $\sim$  TB of storage. This allows only a few runs in three dimensions (3D), and parameter scans for stage optimization can be done in two dimensions (2D) only. Because the size of the box in 3D and the simulation length each scale as  $n_0^{-3/2}$ , a 10 GeV stage at  $n_0 = 10^{17} \text{ cm}^{-3}$  would require  $10^9$  processor-hours which is not yet achievable with today's computational facilities. Approximations are then necessary to simulate such stages at the nominal density and reduced models, such as envelope and quasi-static models [9, 10] or calculation in a Lorentz boosted frame [11, 12, 13], can be used.

The approach used here to design high energy modules is to simulate shorter, higher density stages with scaling of the physical parameters with the plasma density [14]. In the scaled simulations the dimensionless parameters  $k_p L$ ,  $k_p r_0$  and  $a_0$ , where  $k_p = 2\pi/\lambda_p$  is the plasma wave number,  $L$  and  $r_0$  are the laser length and spot size respectively, and  $a_0 = 7.2 \times 10^{-19} \lambda^2 [\mu\text{m}] I [\text{W}/\text{cm}^2]$  is the normalized laser intensity, are kept constants. PIC simulations in the quasi-linear regime ( $a_0 \simeq 1$ ) at different densities and comparison with a quasi-static code in 2D cylindrical geometry at  $n_0 = 10^{17} \text{ cm}^{-3}$  show that the wake structure stays constant under these conditions [15]. Simulations also show that laser evolution, self-focusing and depletion, and electron beam dephasing scale as predicted by the linear theory, even though this theory is strictly valid in the low intensity limit ( $a_0 \ll 1$ ), thus allowing scaled design of multi-GeV stages. Reduction of wake amplitude due to the presence of a charged beam (beam loading) also scales predictably for a wide range of parameters, allowing prediction of beam charge in unscaled stages [14]. Fig. 1(a) shows the accelerating wake structure at  $n_0 = 10^{18} \text{ cm}^{-3}$

\* The author acknowledge the assistance of the VORPAL development team. Work supported by the U.S. Department of Energy, HEP Contract No. DE-AC02-05CH11231, and the COMPASS SciDAC project, and by NA-22, and used computational facilities at NERSC.

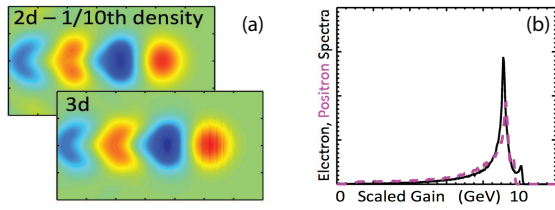


Figure 1: (a) Accelerating field of a scaled stage in 2D at  $n_0 = 10^{18} \text{ cm}^{-3}$  and in 3D at  $n_0 = 10^{19} \text{ cm}^{-3}$  with an electron beam located in the first wave bucket after the driver. (b) Momentum spectrum of an electron (solid line) and positron (dashed line) beam for  $a_0 = 1$ ,  $k_p L = 2$ ,  $k_p r_0 = 5.3$ ,  $n_0 = 10^{19} \text{ cm}^{-3}$  initially on axis followed by a longitudinal linear increase (plasma taper), and beam parameters  $k_p \sigma_{LRMS} = 0.5$ ,  $k_p \sigma_{RMS} = 1$  and  $Q = 22.8 \text{ pC}$  (corresponding to  $Q = 228 \text{ pC}$  at  $n_0 = 10^{17} \text{ cm}^{-3}$ ).

in 2D and  $n_0 = 10^{19} \text{ cm}^{-3}$  in 3D with an electron beam of transverse size  $k_p \sigma_{RMS} = 1.78$  and of charge 130 pC and 50 pC respectively, corresponding to the same amount of beam loading, located in the first wave bucket after the driver. Fig 1(a) shows that the accelerating structure is preserved for different densities and also between 2D and 3D. 2D simulations at  $n_0 = 10^{19} \text{ cm}^{-3}$  can then be used at low cost for optimization of the electron beam shape and longitudinal plasma profile to reduce the energy spread and increase the acceleration length [14], showing that it is possible to accelerate a beam to 10 GeV, with 4% energy spread in 0.7 m, as seen in Fig. 1(b). Because the wake is quasi-symmetric in this regime, positrons can be accelerated in a similar way with the same energy gain and energy spread, also shown in Fig. 1(b). Simulations with various pulse lengths, keeping the laser energy constant, show that efficient stages are obtained at  $k_p L = 1$ , where the laser depletes most of its energy at the dephasing length [15], allowing for 30% more beam charge at the same energy gain. Hence, we were able to increase the efficiency of the stage compared to the initial point design by using scaled PIC simulations, which allows propagation of the laser pulse until depletion.

In the quasi-linear regime, the transverse size of the bunch must be matched to the focusing fields to prevent oscillation of the beam spot size, which can degrade emittance and energy spread [16]. Past simulations used gaussian laser modes, which produce high transverse fields and hence small matched beam sizes. The matched beam spot size, i.e. with no transverse oscillation of the beam, depends on the focusing force strength and is typically of the order of a fraction of a micron for  $n_0 = 10^{17} \text{ cm}^{-3}$ ,  $\gamma = 2 \times 10^4$  and  $\epsilon_n = 1 \text{ mm mrad}$ , where  $\gamma$  is the relativistic factor and  $\epsilon_n$  the normalized emittance of the electron beam. This small spot size, in turn, limits beam charge, and hence stage efficiency, because high charge density creates a blow out disrupting the wake strongly. In the linear or quasi-linear regime ( $a^2 \lesssim 1$ ) the transverse field is directly

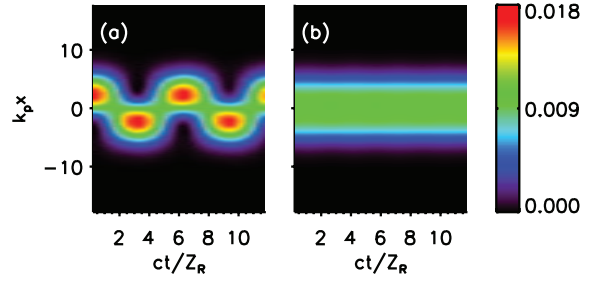


Figure 2: Transverse intensity profile, integrated longitudinally, as a function of propagation distance for the fundamental and first order Hermite-Gaussian mode with parallel (a) and cross (b) polarization, propagating in a matched plasma channel with a density on axis  $n_0 = 10^{19} \text{ cm}^{-3}$ , with  $a_0 = 0.1$ ,  $a_1 = a_0/\sqrt{2}$  and  $k_p L = 2$  and  $k_p r_0 = 5.3$  for both modes.

proportional to the transverse gradient of the laser intensity profile,  $E_{\perp} \sim \nabla_{\perp} a^2$ . It is then possible to reduce the focusing forces, and hence increase the matched beam spot size and the beam charge, by tailoring the transverse profile of the laser pulse.

The transverse laser intensity profile can be shaped by using combinations of higher order laser modes. Solutions of the paraxial wave equation, describing the evolution of the slow varying transverse envelope  $\hat{a}_{\perp}$  of a low intensity ( $|\hat{a}_{\perp}|^2 \ll 1$ ) laser pulse propagating in a matched plasma channel, expressed in the cartesian coordinate system  $(x, y, z)$  are of the form:

$$\hat{a}_{x,(m,p)}(x, y, z) = \frac{a_{m,p}}{(2^{m+p} m! p!)^{1/2}} \times H_m \left( \sqrt{2} \frac{x}{r_0} \right) H_p \left( \sqrt{2} \frac{y}{r_0} \right) \times e^{-(x^2+y^2)/r_0^2 + i\theta_{m,p}} \quad (1)$$

where  $H_m$  are the Hermite polynomials,  $r_0$  is the laser spot size and  $\theta_{m,p} = (-1/2k)[k_p^2 + 4(m+p+1)/r_0^2]z$ ,  $k = 2\pi/\lambda$ , is the phase shift. In solving the paraxial wave equation one can find that the condition for the laser pulse to be matched, i.e., to have no spot size variation, is to propagate in a plasma channel of the form  $n(r) = n_0 + \Delta n_c r^2/r_0^2$ , with  $\Delta n_c = 1/\pi r_e r_0^2$  where  $r_e$  is the classical electron radius [17]. This condition is independent of the mode number: hence, several modes can be propagated in the same plasma channel. On the other hand the phase velocity  $\beta_{ph} \simeq 1 - (1/k)\partial\theta_{m,p}/\partial z$  depends on the mode number, inducing a modulation of the intensity profile with propagation distance when adding two modes with the same polarization. This is shown in Fig. 2(a) where addition of the fundamental and first order Hermite-Gaussian modes with parallel polarization causes the transverse intensity profile to oscillate at the frequency  $k_{\text{beat}} = 1/Z_R$ , where  $Z_R = kr_0^2/2$  is the Rayleigh length. This can be avoided by using orthogonal polarization between the two modes, as shown in Fig. 2(b). For sim-

plicity we used 2D simulations, for which  $\hat{a}_{x(m)}(x, z) = (a_m/\sqrt{2^m m!})H_m(\sqrt{2}x/r_0)\exp(-x^2/r_0^2 + i\theta_m)$ , and  $\theta_m = (-1/2k)[k_p^2 + 2(2m+1)/r_0^2]z$ . Generalization to 3D is straightforward and presented in detail elsewhere [18].

In 2D, when adding the fundamental ( $m = 0$ ) and first order ( $m = 1$ ) Hermite-Gaussian mode with crossed polarization, the intensity profile is of the form:

$$\hat{a}(x)^2 = a_0^2 e^{-2x^2/r_0^2} \left(1 + \frac{4a_1^2 x^2}{a_0^2 r_0^2}\right) \quad (2)$$

Considering a gaussian profile longitudinally,  $\hat{a}(\zeta, x)^2 = \hat{a}(x)^2 \exp(-2\zeta^2/L^2)$ , where  $\zeta = z - ct$  and  $L$  is the laser pulse length, the linear plasma response behind the driver is given by [1]:

$$\phi = -\hat{a}(x)^2 \sqrt{\pi/2}(k_p L/4)e^{-k_p^2 L^2/8} \sin(k_p \zeta) \quad (3)$$

where  $\phi = e\Phi/mc^2$  is the normalized electric potential and  $|\hat{a}|^2 \ll 1$  is assumed. The transverse electric field is then given by  $E_x/E_0 = -(1/k_p)\nabla_x \phi$ , where  $E_0 = mc^2 k_p/e$  is the cold non-relativistic wavebreaking limit, i.e.,

$$\begin{aligned} \frac{E_x}{E_0} &= a_0^2 \sqrt{\pi/2}(k_p L/4)e^{-k_p^2 L^2/8} e^{-2x^2/r_0^2} \frac{4x}{k_p r_0^2} \\ &\times \left(1 - \frac{2a_1^2}{a_0^2} + \frac{4a_1^2 x^2}{a_0^2 r_0^2}\right) \sin(k_p \zeta) \end{aligned} \quad (4)$$

We see that the transverse field is 0 near axis ( $x^2/r_0^2 \ll 1$ ), for all phases  $k_p \zeta$ , for  $a_1/a_0 = 1/\sqrt{2}$ , corresponding to a flat top profile near axis of the intensity profile [Fig. 3(a)].

When the laser pulse is propagating in a plasma channel one has to take into account the curvature of the fields transversely. This can be evaluated to first approximation, assuming a broad channel  $k_p^2 r_0^2 \gg 1$ , by using  $k_p(x) = k_{p0} \sqrt{1 + \Delta n x^2/n_0 r_0^2}$  in eq. (3) [19]. Assuming  $\Delta n_c x^2/n_0^2 r_0^2 = 4x^2/k_p^2 r_0^4 \ll 1$  the transverse electric field can be expressed, to the first order in  $x/r_0$ ,

$$\begin{aligned} \frac{E_x}{E_0} &= \frac{-a_0^2 L}{4r_0} \sqrt{\frac{\pi}{2}} e^{-2x^2/r_0^2} e^{-k_p^2 L^2/8} \\ &\times \left[ \left(4 - \frac{\Delta n}{n_0} + \frac{k_p^2 L^2}{4} \frac{\Delta n}{n_0} - 8 \frac{a_1^2}{a_0^2}\right) \sin(k_p \zeta) \right. \\ &\left. - \frac{\Delta n}{n_0} k_p \zeta \cos(k_p \zeta) \right] \frac{x}{r_0} + \mathcal{O}(x^3/r_0^3) \end{aligned} \quad (5)$$

Contrary to the solution with a flat plasma profile there is no value of  $a_1/a_0$  that gives a null transverse field for all phases, as shown in Fig. 3(a) for  $a_0 = 0.1$ . However we can reduce the transverse field to 0 over a small length of phase if we consider the response of the fundamental and the first order Hermite-Gaussian mode separately and by noticing that the transverse fields driven by each of these modes do not cross the axis at the same phase. By introducing a delay ( $k_p \zeta_s$ ) between the two modes and by adjusting their relative intensity ( $a_1/a_0$ ), with values derived by setting to 0 the first order term in  $x/r_0$  in eq. (5), the

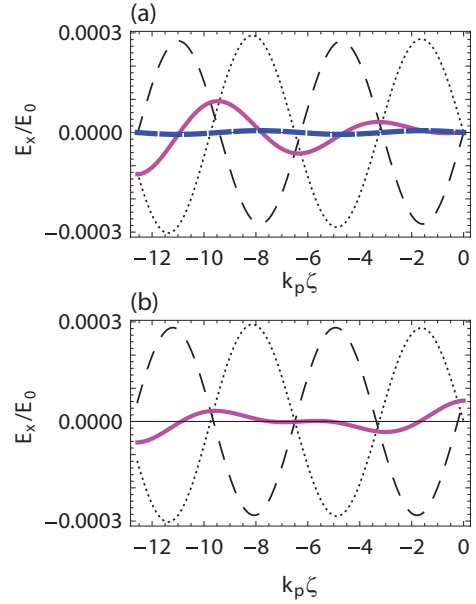


Figure 3: Transverse electric field using higher order modes, as a function of the longitudinal coordinate  $k_p \zeta$  at  $k_p x = 0.1$  and for  $a_0 = 0.1$ ,  $k_p L = 2$  and  $k_p r_0 = 5.3$ . (a) Without (thick dashed line) and with (solid line) including corrections of the plasma channel. Contribution of the fundamental (dotted line) and Hermite-Gaussian mode (thin dashed line), with  $a_1 = a_0/\sqrt{2}$ , in the plasma channel are also shown. (b) The first order Hermite-Gaussian mode is delayed by  $k_p \zeta_s = 0.22$  and the intensity ( $a_1 = 0.72 a_0$ ) adjusted such that the sum (solid line) of the field from the fundamental (dotted line) and the first order mode (dashed line), in the plasma channel, is  $\simeq 0$  around  $k_p \zeta = -6.5$ .

two responses cancel each other and the focusing field can be reduced to 0 over an interval of phase  $k_p \zeta$ , as seen in Fig. 3(b). This produces constant focusing forces over the length of the electron beam and minimizes the field variations as the beam dephases.

PIC simulations show that the two modes can be propagated simultaneously in the same plasma channel with cross-polarization in the quasi-linear regime ( $a_0 \simeq 1$ ), and that the mode does not evolve, i.e., without oscillations. This allows conservation of a reduced transverse field until the laser depletes, as shown in Fig. 4. Injection of a test electron beam shows that the matched beam radius is increased by almost a factor of 3 when using adjusted higher order modes compared to using a gaussian pulse only. Fig. 5 shows the evolution of the beam radius, with normalized emittance  $\epsilon_n = 0.014$  mm mrad ( $k_p \epsilon_n = 6 \times 10^{-3}$ ), accelerated by a plasma wave driven by the fundamental mode only, with  $a_0 = 1$ ,  $k_p L = 1$ ,  $k_p r_0 = 5.3$  and  $n_0 = 5 \times 10^{18}$  cm $^{-3}$ . The electron beam radius oscillates around  $\sigma_x \simeq 0.1$   $\mu\text{m}$  ( $k_p \sigma_x \simeq 0.042$ )  $\pm 30\%$ , while the emittance stays constant, with only 0.01% variation. When adding the first order Hermite-Gaussian mode with  $a_1 = 0.7 a_0$  and a delay of  $k_p \zeta_s = 0.2$ , the matched beam

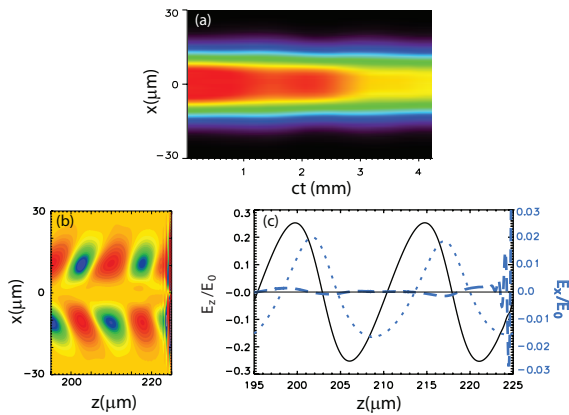


Figure 4: (a) Transverse laser intensity profile, integrated along the longitudinal direction, as a function of the propagation distance, of a fundamental, with  $a_0 = 1$ , plus a first order Hermite-Gaussian mode, with  $a_1 = 0.7$ , delayed by  $k_p \zeta_s = 0.2$ . Both modes verify  $k_p L = 1$  and  $k_p r_0 = 5.3$ , and propagate in a plasma channel with a density on axis  $n_0 = 5 \times 10^{18} \text{ cm}^{-3}$ . (b) Transverse electric field driven by the fundamental plus first order Hermite-Gaussian mode whose transverse profile is shown in (a). (c) Lineout of the transverse field shown in (b) at  $x = 1 \mu\text{m}$  (dashed line) and corresponding accelerating field (solid line). The transverse field driven by the fundamental mode only (dotted line) is also shown.

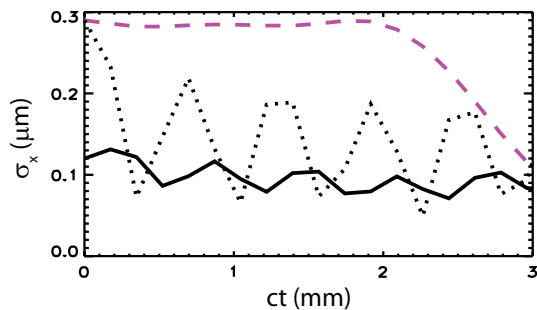


Figure 5: Evolution of a test electron beam spot size in a wakefield driven by the gaussian only, the beam being matched (solid line) and unmatched (dotted line), and in a wakefield driven by the fundamental plus delayed first order Hermite-Gaussian mode (dashed line).

radius is increased to  $\sigma_x \simeq 0.285 \mu\text{m} \pm 1.5\%$  for  $ct < 2$  mm, where the beam slips in a different focusing phase, and has gained 96% of its maximum energy. This represents almost a factor of 3 increase compared to the fundamental mode only, for which a beam with this radius would be highly mismatched (130% variation). This means that we can potentially increase the charge of the bunch (in 3D) by a factor of 9, without increasing the electron beam peak density. The laser power is twice the gaussian case, hence increasing the efficiency by a factor 4.5.

## CONCLUSION

We use PIC simulations for the design of GeV LWFA stages and future 10 GeV modules which will be driven by a 40J-1PW laser system. Stages have been designed in the quasi-linear regime, i.e., moderate laser intensities ( $a_0 \simeq 1$ ), which enables symmetric acceleration of electron and positron beams, advantageous for the high energy particle colliders. We use shorter simulations of stages at higher density and scaling of the physical parameters to predict the behavior of the particle beam in the accelerating structure at reasonable computational cost. This allows us to follow the laser evolution up to depletion for optimization of the stage design.

In the quasi-linear regime, we show that we can tailor the focusing forces acting on the particle beam, by shaping the transverse profile of the laser driver with higher order modes. We show that higher order modes can be propagated simultaneously over many Rayleigh lengths in the same plasma channel, independently of the mode number. However, to avoid intensity modulation due to the difference in phase velocity, cross polarization of the different modes must be used. Linear theory calculations and simulations in the quasi-linear regime show that it is possible to reduce the transverse fields to  $\sim 0$  in the plasma channel by adjusting delay and amplitude of the modes. This allows increase of the matched beam spot size, limited to the region where the fields are linear, of the accelerated electron beam, while keeping the same normalized emittance, enabling increase of the beam charge and stage efficiency important for high energy colliders and gamma ray sources. Future work will include beam loading effects with the use of higher order modes to flatten and reduce the focusing field inside the beam.

## REFERENCES

- [1] E. Esarey *et al.*, Rev. Mod. Phys., 81, (2009), 1229.
- [2] W.P. Leemans *et al.* Nature Phys., 2, (2006), 696.
- [3] J. Faure *et al.*, Nature, 444, (2006), 737.
- [4] A.J. Gonsalves *et al.*, Proc. PAC'09, (2009).
- [5] C.B. Schroeder *et al.*, Proc. AAC Wkshp, 1086, (2009), 637.
- [6] C.G.R. Geddes *et al.*, Proc. CAARI'08 (2008).
- [7] C.B. Schroeder *et al.*, Proc. AAC Wkshp, 1086, (2009), 208.
- [8] C. Nieter and J. Cary, J. Comp. Phys., 196, (2004), 448.
- [9] B. Cowan *et al.*, Proc. AAC Wkshp, 1086, (2009), 309.
- [10] C. Huang *et al.*, J. of Comp. Phys., 217, (2006), 658.
- [11] J.-L. Vay, Phys. Rev. Lett., 98, (2007), 130405.
- [12] J.-L. Vay *et al.*, Proc. PAC'09, (2009).
- [13] S. Martins *et al.*, Proc. PAC'09, (2009).
- [14] E. Cormier-Michel *et al.*, Proc. AAC, 1086, (2009), 297.
- [15] C.G.R. Geddes *et al.*, Proc. PAC'09, (2009).
- [16] P. Michel *et al.*, Phys. Rev. E, 74, (2006), 026501.
- [17] E. Esarey and W.P. Leemans, Phys. Rev. E, 59, (1999), 1082.
- [18] E. Cormier-Michel *et al.*, in preparation.
- [19] N.E. Andreev *et al.*, Phys. Plasmas, 4, (1997), 1145.